Journal of Thermal Analysis, Vol. 41 (1994) 1075-1090

EFFECTS OF ALKALI METAL IONS ON THE THERMAL DECOMPOSITION OF AMMONIUM HEPTAMOLYBDATE TETRAHYDRATE

A. A. Said[1]* *and S. A. Halawy*[2]

[1]Chemistry Department, Faculty of Science, Assiut University, Assiut, Egypt
[2]Chemistry Department, Faculty of Science (Qena), Assiut University, Egypt

(Received July 28, 1992; in revised form May 9, 1993)

Abstract

The thermal decomposition of pure ammonium heptamolybdate tetrahydrate (AHMT), and doped with Li^+, Na^+ and K^+ ions was investigated using thermogravimetry, differential thermal analysis, infrared and X-ray diffraction techniques. Results obtained revealed that the decomposition of AHMT proceeded in three decomposition stages in which both NH_3 and H_2O were released in all stages. The presence of 0.5 mol% alkali metal ions enhances the formation of the intermediate $(NH_4)_2MO_7O_{22}\cdot 2H_2O$ while the decomposition of this intermediate into MoO_3 is slightly affected in the presence of all dopant concentrations used. The infrared absorption spectra of the thermal products of AHMT treated with 10 mol% alkali metal ions (AMI) at 350°C indicated a reduction of some Mo^{6+} ions. By heating of AHMT above 500°C in presence of 5 or 10 mol% of AMI, a solid–solid interaction between alkali metal oxides and MoO_3 giving rise to well crystallized alkali metal molybdates. Finally the activation energies accompanied various decomposition stages were calculated.

Keywords: alkali metal oxides, ammonium heptamolybdate tetrahydrate, DTA, IR, TG, X-ray

Introduction

The thermal decomposition of ammonium heptamolybdate made the subject of several investigations [1–3]. The decomposition process takes place according to different mechanisms depending mainly upon the atmosphere in contact with the solid. The alkali metal oxides are ubiquitous in heterogeneous catalysts, and act as both promoters and poisons. The addition of these oxides to MoO_3 leads to the formation of bronzes depending on their concentration and the atmosphere in contact with the solid [4–7]. The study of the mechanism of

---

* To whom all correspondence should be addressed.

John Wiley & Sons, Limited, Chichester
Akadémiai Kiadó, Budapest

a catalytic process involving a solid catalyst requires a thorough and comprehensive knowledge of the solid body on the surface of which the elementary catalytic event occurs. This knowledge is achieved by the study of the nature and composition of the phases occurring in a system typical of the catalyst, and by investigating the structure and properties of the solid products. However, the thermal decomposition process of ammonium heptamolybdate in the presence of alkali metal oxides have received little attention. The aim of this work was to study the effects of the alkali metal oxides on the thermal decomposition stages of ammonium heptamolybdate. On the other hand, the substances produced from the solid–solid interaction between MoO_3 and the alkali metal oxides are characterized using different techniques. The techniques employed in this work were TG, DTA, X-ray diffraction and IR absorption spectroscopy.

Experimental

Materials

The raw materials used in the present investigation were of AR pure chemical grade. Doping of ammonium heptamolybdate tetrahydrate (AHMT), $(NH_4)_6MO_7O_{24}\cdot 4H_2O$ with Li_2O, Na_2O and K_2O were affected by impregnation from dilute aqueous solutions of carbonate salts (using few drops of nitric acid (1:1), for the ease of dissolution of carbonates) with stirring at room temperature. The impregnated samples were dried in an oven at 110°C to constant weight, then calcined in air at different temperatures. The alkali metal oxide contents, expressed in mol% were 1.5 and 10.

Techniques

Thermogravimetry (TG) and differential thermal analysis (DTA) were carried out using a Shimadzu Computerized Thermal Analysis System DT-40. The system includes programs which process data from the thermal analyzer with the Chromatopac C-R3A. The heating rate was kept at 10 $deg\cdot min^{-1}$ using an atmosphere at a flow rate of 40 $cm^3\cdot min^{-1}$. α–alumina powder was applied as a reference for DTA standard material.

Peak integration and subsequent activation energy calculations were performed using the Shimadzu partial area integration program.

The X-ray diffraction (XRD) of the thermal products of pure (AHMT) and treated with 5 and 10 mol% alkali metal oxides were performed with a Philips diffractometer model (JSK-60PA) JEOL, LTD). The patterns were run with nickel-filtered copper radiation. The diffraction patterns thus obtained were matched with relevant ASTM cards [8] for identification purposes. The infrared absorption spectra (IR) of the thermal solid products were recorded from KBr disc using a Pye Unicam model (Sp3-300) spectrophotometer.

Results and discussion

TG and DTA curves of pure AHMT are shown in Fig. 1. Table 1 gives the maximum temperatures for the decomposition stages together with the activation energy corresponding values. The DTA (curve a) exhibits three decomposition peaks, the maximum of these are located at 123, 220 and 307°C, respectively. The TG (curve b) shows that AHMT loses weight with heating over three steps. The first endothermic peak at 95–150°C was followed by 7.2% mass loss corresponding to the loss of three H_2O molecules and two molecules of NH_3 which is consistent with the theoretical value (7.1%). The second endothermic peak at 190–225°C which was accompanied by a loss of 4.3% is probably related to the elimination of $(NH_4)_2O$ (i.e. $2NH_3$ $+H_2O$) which is in agreement with the theoretical value (4.2%). The third endothermic peak takes place within 267–325°C was associated with 6.8% weight loss (theoretical value 7.1%) and corresponds to the evolution of $(NH_4)_2O$ together with two molecules of H_2O. These three stages can be explained to proceed according to the following equations:

$$(NH_4)_6Mo_7O_{24}\cdot 4H_2O \xrightarrow{95\text{–}150^\circ C} (NH_4)_4Mo_7O_{23}\cdot 2H_2O+3H_2O+2NH_3 \qquad (1)$$

$$(NH_4)_4Mo_7O_{23}\cdot 2H_2O \xrightarrow{190\text{–}225^\circ C} (NH_4)_2Mo_7O_{22}\cdot 2H_2O+H_2O+2NH_3 \qquad (2)$$

$$(NH_4)_2Mo_7O_{22}\cdot 2H_2O \xrightarrow{267\text{–}325^\circ C} 7MoO_3+3H_2O+2NH_3 \qquad (3)$$

The DTA and TG curves (curves b, c and d) of AHMT calcined at 110, 150 and 250°C for 2 h respectively are shown in Fig. 1. These curves indicate that, AHMT calcined at 110–150°C decomposes in two steps while the sample calcined at 250°C proceeds in one decomposition step. The IR spectra of the solid products of the different decomposition stages are shown in Fig. 2. It appears that the samples heated from 110 up to 250°C curves (b, c and d) still contain both water and ammonia. The bands assigned at 1420 and 1630 cm^{-1} corresponds to δOH and δNH_3 respectively. These results support the above mechanism in which the first decomposition step is not only to the dehydration process. Thus the recent investigation differ from the present result in that the first stage of decomposition was a dehydration [1].

Table 1 The maximum decomposition temperature (T_{max} / °C) and the activation energy (E / kJ·mol^{-1}) of pure AHMT and doped with alkali metal ions

Sample	1st stage		2nd stage		3rd stage		4st stage	
	T_{max}	E	T_{max}	E	T_{max}	E	T_{max}	E
AHMT pure	123	219	220	68	307	260	–	–
AHMT +0.5% Li^+	–	–	197	155.7	307	282.8	–	–
AHMT +5% Li^+	–	–	191	79.8	303	191.6	–	–
AHMT +10% Li^+	–	–	186	37	297	128	570	36.4
AHMT +0.5% Na^+	–	–	194	139	306	269.4	–	–
AHMT +5% Na^+	–	–	188	61.7	299	193.5	523	24.7
AHMT +10% Na+	–	–	170	47	$\frac{301}{319}$	123.6	$\frac{523}{539}$	105.4
AHMT +0.5% K^+	–	–	198	157.5	307	251.5	–	–
AHMT +5% K^+	–	–	204	136	300	94.3	540	30.5
AHMT +10% K^+	–	–	216	147	299	80.8	540	60.2

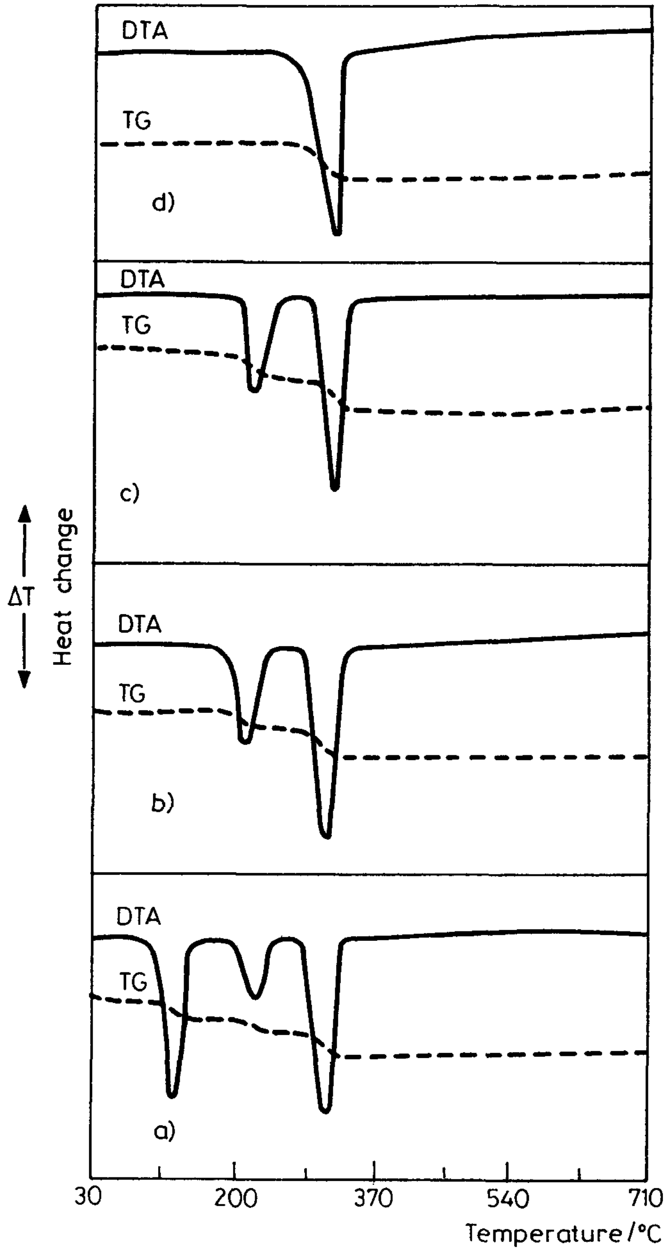

Fig. 1 TG and DTA curves of untreated AHMT (a); calcined for 2 h at 110°C (b); 150°C (c); and 250°C (d)

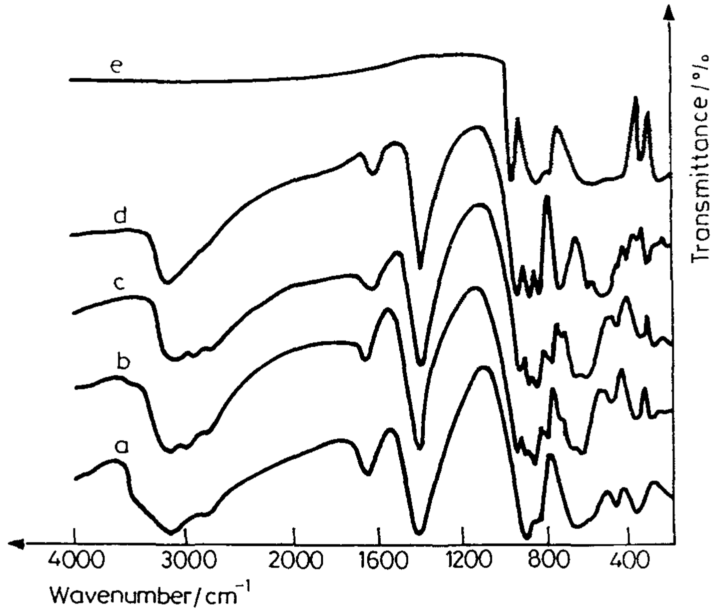

Fig. 2 IR spectra of untreated AHMT (a), calcined for 2 h at 110°C (b), 150°C (c), 250°C (d) and 350°C (e)

On the other hand, our results were in good agreement with the results obtained earlier [2, 9–11], in which they suggested that both H_2O and NH_3 are released at the first stage. Moreover, the IR spectrum of the sample heated at 350°C (curve e) shows the absence of IR bands corresponding to the presence of ammonia and water whereas the significant bands of MoO_3 were observed. The bands lay at 990 and 880 cm^{-1} were attributed to νMo=O and νMo–O–Mo, respectively [12]. In addition, the X-ray diffraction patterns of AHMT calcined at 350° and 500°C revealed that the lines located at d(Å) = 6.93, 3.81, 3.46, 3.25, 2.65, 2.31 and 1.85 are all related to the characteristic lines of MoO_3 crystal lattice [13]. The above results indicated that AHMT decomposes in three stages and MoO_3 is completely exist on heating up to 350°C.

Figure 3 represents the TG and DTA curves of AHMT and AHMT treated with Li^+ ions, Table 1 gives the T_{max} and E of the different decomposition steps. Curve(a) shows that the thermal decomposition of AHMT heated at 110°C for 2 h proceeds in two stages. Curves (b. c and d) of the AHMT doped with 0.5, 5 and 10 mol% Li^+ ions, respectively show the following observations:

i) the first endothermic peak corresponding to the formation of the intermediate, $(NH_4)_2Mo_7O_{22}{\cdot}2H_2O$ is strongly affected in presence of Li^+ ions. The en-

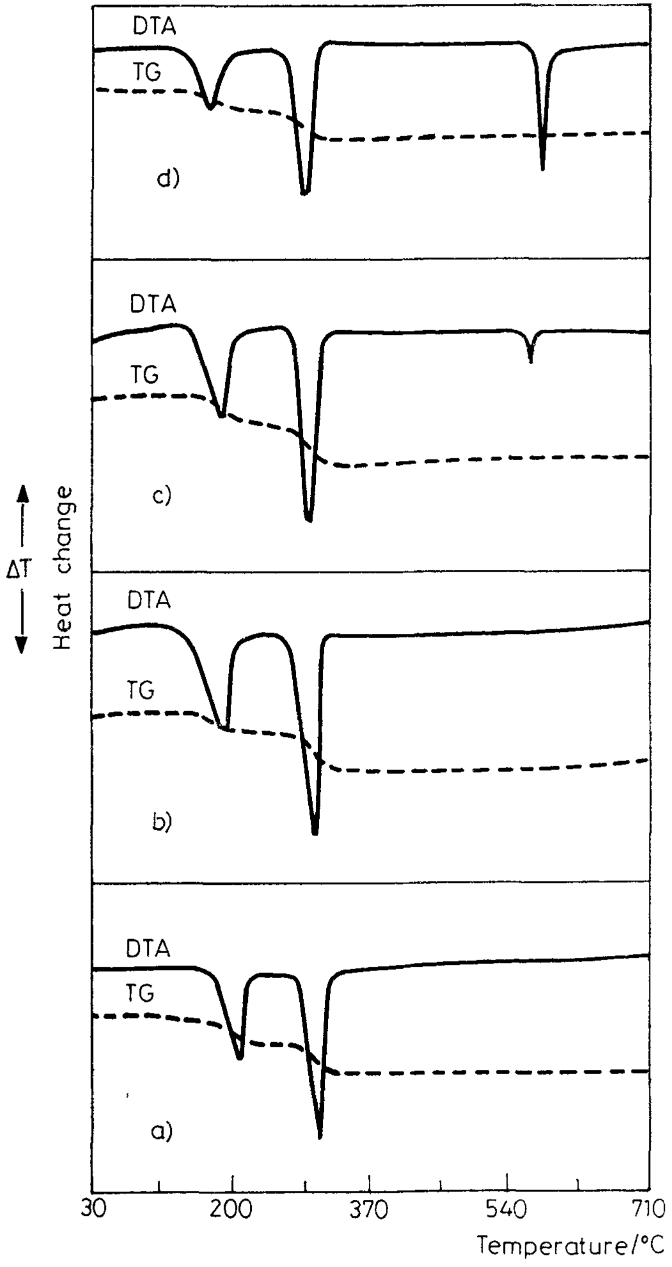

Fig. 3 TG and DTA curves of AHMT (a) and AHMT doped with 0.5 mol% Li^+(b), 5 mol% Li^+(c) and 10 mol% Li^+(d)

hancement effect of the formation of this intermediate depends on the concentration of Li^+ ions;

ii) the endothermic peak of the second stage corresponding to the decomposition of this intermediate is slightly affected in the presence of Li^+ ions;

iii) the new endothermic peak maximised at 570°C (curve c) was not followed by weight loss, and its area increases with increasing the extent of Li^+ ion is most probably attributed to the formation of lithium molybdate spinel, Li_2MoO_4 [14].

Figure 4 represents the DTA and TG curves of AHMT and AHMT doped with 0.5, 5 and 10 mol% Na^+ ions, curves (b, c and d) while T_{max} and E corresponding to the decomposition stages are cited in Table 1. These results concluded that

i) the presence of Na^+ ions leads to a significant change in the decomposition stages of AHMT. The first endothermic peak corresponds to the formation of the intermediate, $(NH_4)_2Mo_7O_{22}\cdot 2H_2O$, shifts to lower decomposition temperature (using up to 10 mol% Na^+ ions);

ii) the decomposition of this intermediate (i.e. the second step) is unaffected in presence of 0.5 mol% Na^+ whereas in presence of 5 or 10 mol% Na^+ ions it proceeds in two endothermic steps. The first peak maximised at 299° and 301°C corresponds to the decomposition of the intermediate existing in the first stage to MoO_3 . The second one maximised at 320°C may be attributed to the reduction [15] of some of Mo^{6+} into Mo^{5+};

iii) the sharp and strong new endothermic peak maximised at 523°C (curves c and d) was not followed by weight loss and its area increases with increasing the content of Na^+ ions may correspond to the formation of sodium molybdate spinel, α–Na_2MoO_4 [16]. Moreover, the endothermic peak located at 540°C as observed in presence of 10 mol% Na^+ is probably due to phase transition of α–Na_2MoO_4 into β–Na_2MoO_4 [16].

Figure 5 shows the DTA and TG curves of AHMT and AHMT treated with 0.5, 5 and 10 mol% K^+ ions while the T_{max} and E values corresponding to the decomposition steps are listed in Table 1. These results can be concluded as follows:

i) the addition of 0.5 mol% K^+ ions enhances the first decomposition stage of AHMT whereas the second step is unaffected;

ii) in presence of 5 or 10 mol% K^+ ions, the enhancement of the AHMT first stage decreases while it enhances the decomposition of the second stage;

iii) the new sharp and strong endothermic peak maximised at 540°C accompanied without weight loss and its area increases with increasing the content of

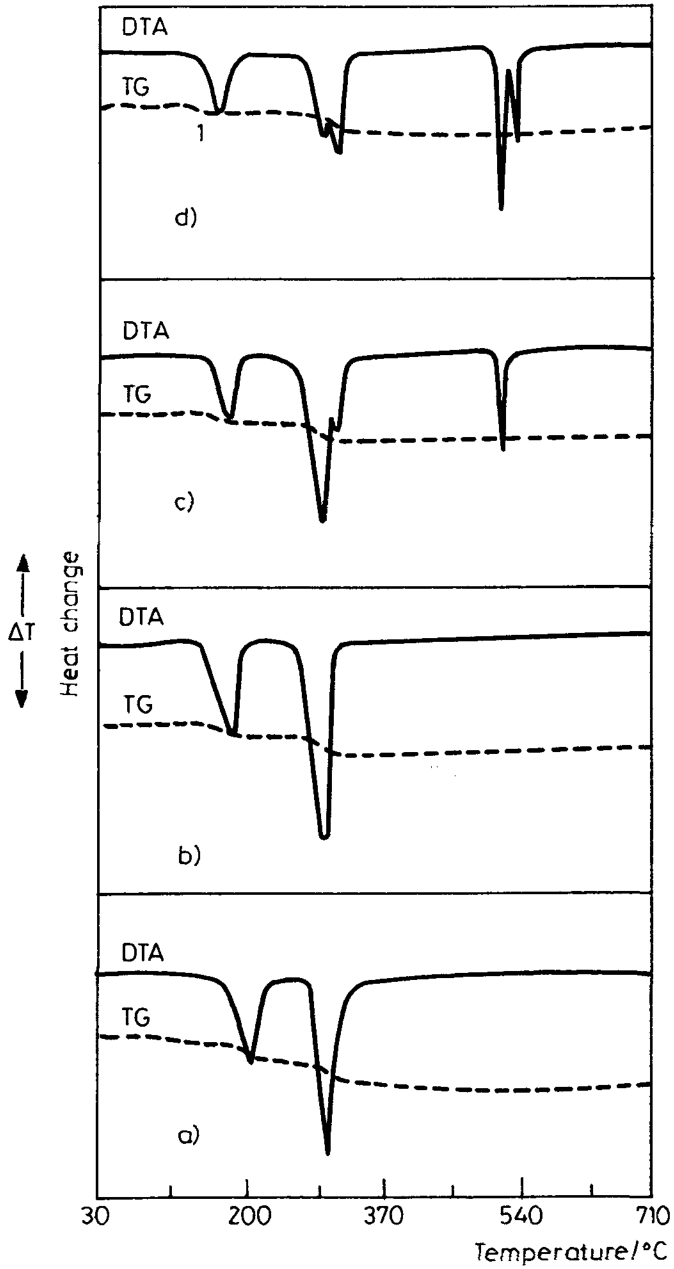

Fig. 4 TG and DTA curves of AHMT (a) and AHMT doped with 0.5 mol% Na^+(b), 5 mol% Na^+(c) and 10 mol% Na^+(d)

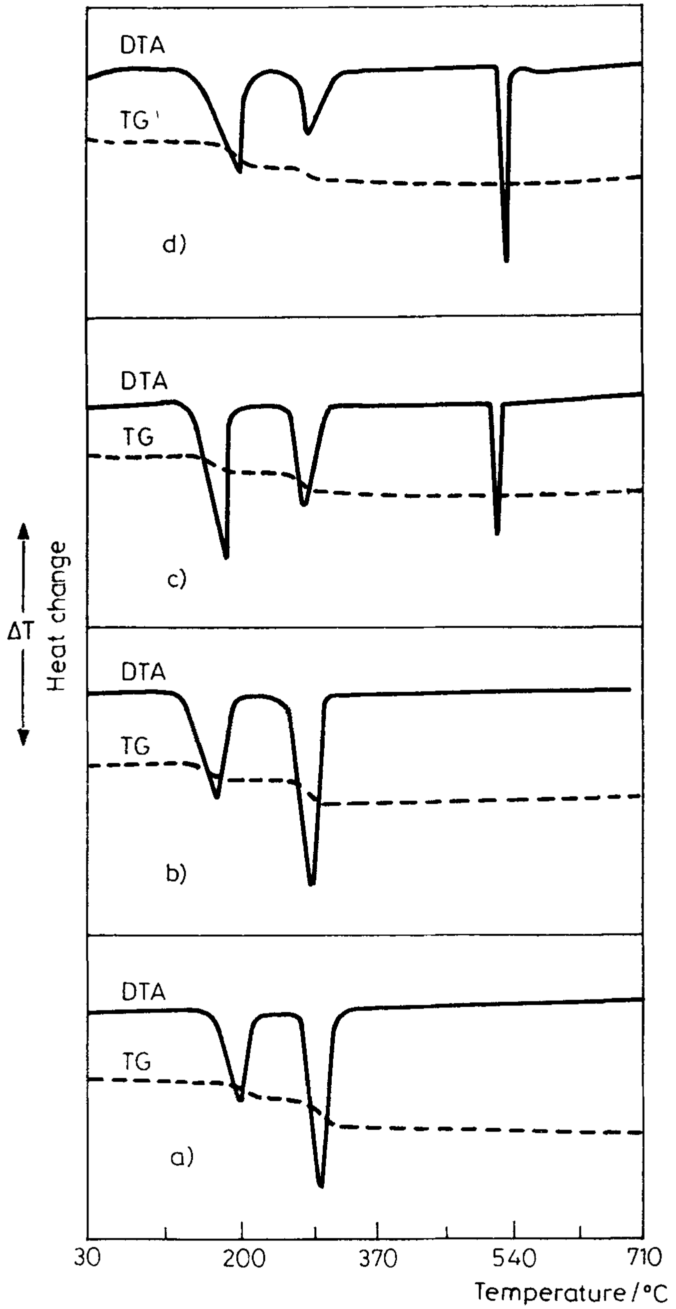

Fig. 5 TG and DTA curves of AHMT (a) and AHMT doped with 0.5 mol% K^+(b), 5 mol% K^+(c) and 10 mol% K^+ (d)

K^+ ions may correspond the formation of potassium molybdate spinel, K_2MoO_4 [17].

The IR spectra of AHMT and AHMT treated with 10 mol% Li^+, Na^+ and K^+ calcined at 350°C for 2 h given (Fig. 6).

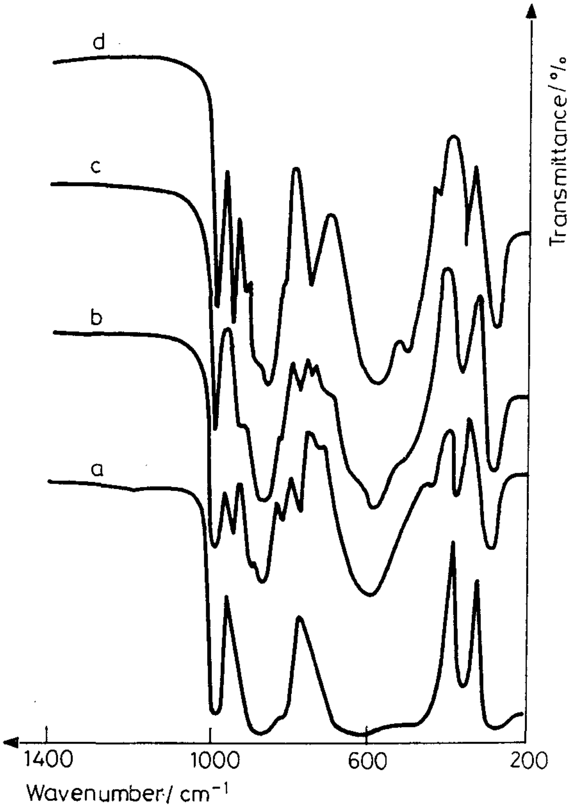

Fig. 6 The IR absorption spectra of solid products at 350°C for pure AHMT (a) and doped with 10 mol% Li^+ (b), 10 mol% Na^+(c) and 10 mol% K^+ (d)

These spectra show a significant change in the vibration bands characteristic of MoO_3 (curve a). These changes support that, the presence of various additives strongly affected the crystal lattice of MoO_3. The observed new bands assigned at 970, 780 and 720 cm^{-1} are probably due to the lower valence of molybdenum oxide or the decrease in the bond strength of Mo–O [18]. Consequently, these results clearly point that the dissolution of the dopant cations in the oxide lattice may proceed via location in the cationic vacancies, interstitial positions of the MoO_3 lattice. The location of Li^+, Na^+ or K^+ ions in cationic vacancies or interstitial positions in MoO_3 solid should be accompanied by a decrease in the concentrations of Mo^{6+} ions [19] according to

$$M_2O + 2Mo^{6+} \longrightarrow 2M\boxed{\Delta} + Mo^{5+} + 0.5\ O_2 \qquad (4)$$

where $\boxed{\Delta}$ is lithium, sodium or potassium ions located in cationic vacancies or in interstitial positions. The dissolution of alkali metal according to such a mechanism is accompanied by degassing of some excess oxygen O_2 followed by subsequent transformations of some Mo^{6+} into Mo^{5+} ions. It is important to mention that the creation of Mo^{5+} ions should decrease the ratio of Mo^{6+}/Mo^{5+} ions which plays a decisive role in the catalytic reactions. However, the reduction of some Mo^{6+} into Mo^{5+} was found to be responsible for retardation of the dehydration activity of MoO_3 towards isopropyl alcohol [20]. The IR spectra of solid products of AHMT and AHMT treated with 10 mol% Li^+, Na^+ or K^+ ions and calcined at 600°C for 4 h are shown in Fig. 7. It can be seen that the 990 cm^{-1} band in the MoO_3 spectrum (curve a) corresponding to Mo=O is assigned for all samples. The appearance of such a band confirms the presence of MoO_3 together with spinels formed. The noticeable change in the spectra of these solids is observed in the range of 950–500 cm^{-1}. This change is accom-

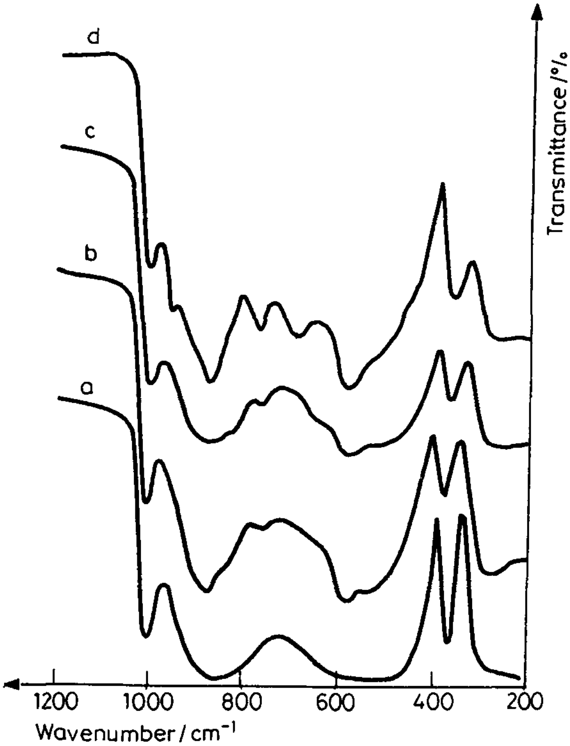

Fig. 7 The IR absorption spectra of the solid product for AHMT (a) and doped with 10 mol% Li^+ (b), 10 mol% Na^+(c) and 10 mol% K^+ (d) after firing at 600°C

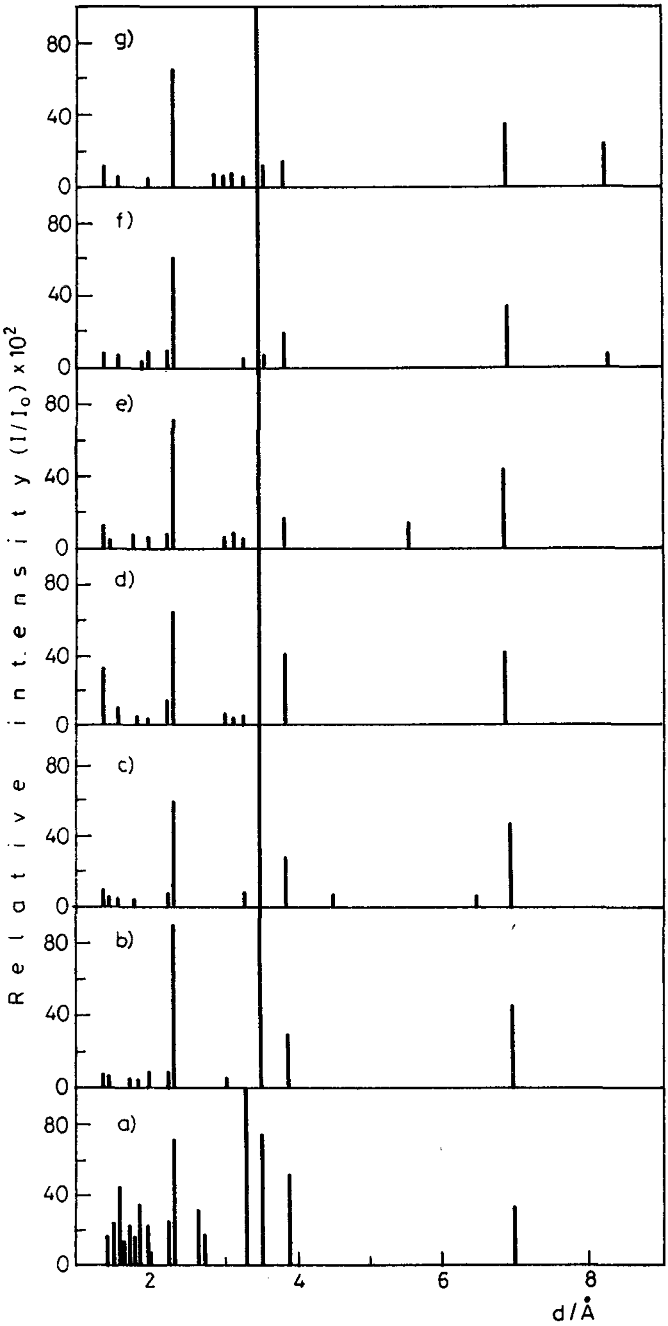

Fig. 8 The X-ray diffraction patterns of the solid products at 600°C of AHMT (a) and doped with 5 and 10 mol% (b and c), 5 and 10 mol% Na^+ (d and e) and 10 mol% K^+ (f and g), respectively after firing at 600°C

pained with the absorption of new bands at 950, 770, 690 and 580 cm^{-1} which may be corresponded to the formation of alkali metal molybdates.

Figure 8 shows the X-ray diffraction patterns of AHMT and AHMT treated with 5 and 10 mol% Li^+, Na^+ or K^+ ions and that calcined at 600°C for 4 h (Patterns a–g respectively). Pattern (a) shows the characteristic lines of MoO_3 which are detected in the XRD patterns of AHMT calcined at 330° and 500°C. The addition of 5 or 10 mol% of the alkali metal oxides, cause the appearance of strong diffraction lines at $d(Å) = 3.47$ corresponding to I/I_o = together with linesat $d(Å) = 6.92, 3.8, 2.31$ corresponding to unreacted MoO_3 diffraction lines. Therefore, the endothermic peaks observed in the DTA curves (Figs 2–4) at a temperature >500°C for samples containing 5 and 10 mol% of alkali metal oxides gave the corresponding molybdates due to the solid–solid interaction between MoO_3 and M_2O (M = Li^+, Na^+ or K^+). This reaction can be proceeded according to the following equation:

$$M_2O + MoO_3 \xrightarrow{>500\ ^{\circ}C} M_2MoO_4 \qquad (5)$$

It is known that the ionic radii of Li^+, Na^+, K^+ and Mo^{6+} ions are 0.60, 0.97, 1.33 and 0.62 Å, respectively. However, the observed decrease in the peak area corresponding to the formation of lithium molybdate compared with other dopants can be explained on the basis that the main part of Li^+ ions was effectively dissolved in MnO_3 lattice and a small part of the dopant underwent a solid–solid interaction with MoO_3 producing a new phase of lithium molybdate. Finally, Table 1 indicates that the activation energies accompanied the decomposition of the intermediate $(NH_4)_4Mo_7O_{22}\cdot 2H_2O$ and $(NH_4)_2Mo_7O_{21}\cdot 2H_2O$ in presence of 0.5 mol% alkali metal ions increased in the direction:

$$Li^+ > Na^+ > K^+$$

On increasing the percentage dopants an observable decrease in the E values accompanied the decomposition of the two stages.

Conclusions

The main conclusions that can be derived from the experimental results are as follows:

1. the decomposition of AHMT proceeds in three decomposition steps in which both ammonia and water are released in all decomposition steps;

2. the addition of low percentage of alkali metal ions enhances the formation of the intermediate: $(NH_4)_2MO_7O_{22}\cdot 2H_2O$, while the decomposition of this intermediate is slightly affected in presence of low and high concentration;
3. the IR spectra of the thermal products of AHMT treated with 5 or 10 mol% at 350°C indicated a reduction of some Mo^{6+} into Mo^{5+} ions.
4. by heating of AHMT in presence of 5 and 10 mol% alkali metal ions above 500°C, a solid–solid reaction has been occurred giving alkali metal molybdates. The formation of these spinels is found to depend on the ionic radii of the dopant ion;
5. the activation energies accompanied for the decomposition stages of AHMT are strongly affected in the presence of alkali metal ions.

References

1 W. J. Young, Thermochim. Acta, 158 (1990) 183.
2 K. Isa, Y. Hirai and H. Ishimura, Proc. ICTA-5, Tokyo 1977, p. 348.
3 M. Onchi and E. Ma, J. Phys. Chem., 67 (1963) 2240.
4 M. Greenblatt, K. V. Ramanujachary, W. H. McCaroll, R. Neifeld and J. V. Waszczak, J. Solid State Chem., 59 (1985) 149.
5 T. Hiratta and Y. Fukuda, J. Mat. Sci. Lett., 9 (1990) 929.
6 A. C. W. P. James and J. B. Goodenough, J. Solid State Chem., 76 (1988) 87.
7 A. K. Gangule, L. Ganapathi, J. G. A. Krishnan and C. N. R. Rao, J. Solid State Chem., 74 (1988) 228.
8 W. F. McClune (Ed.), Powder Diffraction File (Inorganic Compounds), JCPDS, PA (1978).
9 E. Ma, Bull. Chem. Soc. Jpn., 37 (1964) 649.
10 K. Manaba, M. Ogawa, Y. Yonemura and T. Kubo, Nippon Kagaku Kaishi, 7 (1977) 947.
11 Z. M. Hanafi, M. A. Khilla and M. H. Askar, Thermochim. Acta, 45 (1981) 221.
12 S. R. Seyedonir, S. Abdo and R. F. Howe, J. Phys. Chem. Lett., 86 (1982) 233.
13 G. Alessandrini, L. Catrati, P. Forzatti, P. L. Villa and F. Trifiro, J. Less-Common Metals, 54 (1977) 373.
14 W. S. Brown, H. S. Parker, R. S. Roth and J. L. Woring, J. Cryst. Growth, 16 (1972) 118.
15 N. K. Kapustkin, R. N. Plentov, L. Volkov and A. A. Forteiv, Khim. Teknol. Ven. Soedin Mater. Vses Soveshist (1972) 299.
16 Zh. G. Bazarova, S. I. Arkhincheeva and M. V. Mokhosoev, Izv. Akad. Nauk SSSR, Neorg. Mater., 17 (1981) 1868.
17 Gaillet, Bull. Soc. Chim. Fr., 12 (1967) 4751.
18 M. Akimoto and E. Echigoya, J. Catal., 35 (1974) 278.
19 A. Bielanski, J. Deren and J. Haber Sloczinski Trains, Faraday Soc., 58 (1962) 166.
20 A. A. Said, Int. J. Chem., 3 (1992) 47.

Zusammenfassung — Mittels TG, DTA, IR- und Röntgentechniken wurde die thermischer Zersetzung von reinem sowie mit Li^+-, Na^+- und K^+-Ionen versetztem Ammoniumheptamolybdat-Tetrahydrat (AHMT) untersucht. Die Ergebnisse zeigten, daß die Zersetzung des eingesetzten AHMT in drei Zersetzungsschritten abläuft, bei denen in allen dreien sowohl NH_3 als auch H_2O freigesetzt wird. Die Anwesenheit von 0.5 mol% Alkalimetallionen steigern die

Bildung des Zwischenproduktes, während die Zersetzung dieses Zwischenproduktes zu MoO_3 in Gegenwart aller verwendeten Zusatzkonzentrationen nur geringfügig beeinflußt wird. Das IR-Absorptionsspektrum der thermischen Produkte von AHMT, was bei 350°C mit 10 mol% Alkalimetallionen (AMI) behandelt wurde, zeigte die Reduktion einiger Mo^{6+}-Ionen. Beim Erhitzen von AHMT über 300°C in Gegenwart von 5 oder 10 mol% AMI führt eine Feststoff-Feststoff-Wechselwirkung zwischen Alkalimetalloxiden und MoO_3 zu sehr gut kristallisierten Alkalimetallmolybdaten. Letztlich wurden die Aktivierungsenergien der verschiedenen Zersetzungsschritte berechnet.